Journal of Thermal Analysis and Calorimetry (2019) 138:359–368
https://doi.org/10.1007/s10973-019-08230-8

Capric acid/intercalated diatomite as form-stable composite phase change material for thermal energy storage

Peng Liu[1] · Xiaobin Gu[1,2,3] · Liang Bian[1,4] · Lihua Peng[5] · Huichao He[2]

Received: 15 October 2018 / Accepted: 1 April 2019 / Published online: 13 April 2019

Abstract
Leakage issue and low thermal conductivity largely restrict feasibility of fatty acid in real application of thermal energy storage (TES). In this paper, a novel form-stable phase change material (FSPCM) capric acid/diatomite (CA/DT) for TES was prepared using direct impregnation method by using CA as PCM and diatomite as supporting material. The fabricated composites were investigated in detail via the leakage test to determine the optimization proportion, and the real mechanism of preventing leakage by diatomite was analyzed. The characterization techniques such as thermogravimetric analysis, differential scanning calorimetry, intelligent paperless recorder technology, Fourier transform infrared spectrometer and scanning electron microscopy were applied to systematically investigate the thermal properties, microstructure and thermal compatibility of the prepared composites. The results showed that the maximum mass ratio of CA adsorbed into DT without leakage is as high as 50 mass%, which is mainly ascribed to the porous structure of DT. The selected FSPCM has a melting point of 34.9 °C and latent heat of 89.2 J g^{-1}. What is more, the CA/DT FSPCM exhibits a distinctly enhanced thermal stability by TG analyses. The heat transfer efficiency of the CA/DT FSPCM is higher than that of pristine CA. Due to the high adsorption capacity, high latent heat, good thermal stability as well as low cost, the CA/DT FSPCM can be considered as potential materials for thermal energy storage.

Keywords Form-stable phase change materials · Capric acid · Diatomite · Building energy conservation · Thermal energy storage · Leakage

Introduction

Recently, thermal energy storage technology for energy conservation, which aims to increase the efficiency of energy use, is playing more and more important role in dealing with the energy shortages and environment problems. The thermal energy technology contains sensitive heat storage, latent heat storage and chemical reaction heat storage. In comparison with other heat storage technology, latent heat storage using phase change materials (PCMs) is considered to be the more promising way to increase the energy efficiency in lots of application fields, owing to the high latent heat capacity and small temperature variation during phase change process [1, 2]. Among the PCMs, fatty acids are a particular important class of PCMs for thermal energy storage (TES) due to their good properties. For example, capric acid (CA) is one of the typical representatives and taken as a promising PCM because of its proper phase change temperature, high latent heat capacity, almost

✉ Peng Liu
hgump@hgu.edu.cn

✉ Xiaobin Gu
XBGu@hgu.edu.cn

1 College of Gems and Materials Technology, Hebei GEO University, Shijiazhuang 050031, Hebei, China

2 State Key Laboratory for Environment-Friendly Energy Materials, South West University of Science and Technology, Mianyang 621010, Sichuan, China

3 Material Corrosion and Protection Key Laboratory of Sichuan Province, Zigong 643000, Sichuan, China

4 Key Laboratory of Solid Waste Treatment and Resource Recycle, Ministry of Education, South West University of Science and Technology, Mianyang 621010, China

5 Key Laboratory of Orogenic Belts and Crustal Evolution, MOE, School of Earth and Space Sciences, Peking University, Beijing 100871, China

no supercooling during the phase transition, no phase separation, good chemical and thermal stability after long-term utility period, low vapor pressure, congruently melting, non-toxicity and non-corrosivity against metal containers [3–5]. However, direct use of these kinds of PCMs tends to have some drawbacks such as undesirable leakage, erosion and instability, which strongly limit the further applications of PCM. In order to overcome the above-mentioned leakage problem, a great deal of efforts have been made to improve the encapsulation technology, which primarily include nano-encapsulating pure PCM [6–9] and impregnating pure PCM into the porous minerals, such as kaolinite [10, 11], graphite [12–14], perlite [15], meteorite [16] and diatomite [12, 17–19]. In particular, it is noted that employing porous minerals by composite methods to develop, such as FSPCM, has shown great potential as effective solutions since mineral PCMs have many advantages over other methods. For example, it can greatly enlarge heat transfer area, prevent PCMs from leaking and reduce influences of outside environment. Therefore, some attempts have recently been made to investigate the composite technologies by impregnating PCMs into porous structure of porous minerals [20–23].

Among the above-mentioned porous minerals, diatomite (DT) is a type of natural porous mineral, which has many excellent properties such as good chemical stability, prominent pore structure, significant specific surface area, high absorptivity, high purity and relatively low price. Thus, DT is considered to be a feasible candidate as an economical support material for incorporating CA as the PCM for thermal energy storage. Particularly, the physical structure and chemical composition of DT make it support PCM and become a hot spot in shape-stabilized PCM research [24–27]. As far as we know, CA/DT FSPCM has not been fabricated and characterized in any other literature till now.

In this article, a novel CA/DT FSPCM was prepared via the direct impregnation method in the air by absorbing CA into the DT, which restricts CA from leaking during the phase change process. The leakage properties of this novel FSPCM were systematically investigated by the leakage test. At the same time, the thermal properties, chemical compatibility and microstructure of FSPCM were characterized by virtue of different analysis techniques.

Experimental

Materials

Capric acid (CA, 98.5% pure) was purchased from Sinopharm Chemical Reagent Co., Ltd. (Shanghai, China). The diatomite sample was supplied by China's Damao Chemical Reagent Co., Ltd. (Tianjin, China). The diatomite samples were dried at 120 °C for 2 h to remove existing water.

Preparation of CA/diatomite PCM composite

The CA/DT composites were prepared via direct impregnation method [2, 27, 28]. Firstly, CA and DT were weighed according to different ratios (1:0, 8:2, 7:3, 6:4, 5:5, 4:6, 3:7) and mixed evenly in a 250-mL beaker. Secondly, the mixture in the beaker was put in the water bath at a constant temperature of 60 °C, which is higher than phase change point of 31.5 °C, until it melted completely, and then, the liquid PCM was impregnated into porous space of DT. Thirdly, the melted CA/DT composites were stirred using a magnetic stirring apparatus at 50 rpm for 10 min. In addition, the other samples were successively fabricated according to the above procedures. At last, all the prepared samples were dried at room temperature for further use. The better absorption ratio, i.e., the maximum capacity without leakage of CA in DT, can be determined by the leakage test. All samples are marked according to Table 1 in this paper.

Characterization of CA/DT composites

The morphology of CA, DT and CA/DT FSPCM was examined by scanning electron microscope (SEM, Phenom ProX, Netherlands). The FTIR spectra were recorded by Fourier transform infrared spectrometer (FTIR, Thermo Scientific, USA). The wavenumber region of FTIR spectra ranged from 400 to 4000 cm^{-1}. The thermal properties of CA and CA/DT were studied by differential scanning calorimeter (DSC, TA, Q100, USA). The testing temperature was between 0 and 70 °C, whose heating rate was 10 °C min^{-1}. The thermal stability of CA and CA/DT FSPCM was tested by a thermal gravimetric analyzer instrument (TG, TA, Q600, USA), and the operating temperature ranged from 25 °C (the room temperature) to 600 °C with a heating rate of 20 °C min^{-1}. The cooling curve of CA and CA/DT composites was investigated by intelligent paperless recorder, which can record the temperature variations of the CA/DT mixtures. In order to investigate the thermophysical properties of CA/DT composites, 10 g composite for each sample was loaded into the centrifuge tube, and the temperature ranged from − 10 to 60 °C for the heating process and 60 to − 10 °C for the cooling process. During the whole process, the temperature data were recorded by the paperless logger.

Leakage issue in melting state seriously restricts feasibility of fatty acid in real application of TES. Therefore, the leakage tests and the mechanism of preventing PCM leakage were investigated in detail. However, at present,

Table 1 Basic proportion and corresponding leakage data of the CA/DT composites

Step	Sample name	The composition ratio of the CA/DT composite	Leakage ratio/%	Leakage area of the sample/cm^{-2}
1	S1-1	Pure CA	77.57	31.36
1	S1-2	80% CA + 20% DT	31.23	24.01
1	S1-3	70% CA + 30% DT	10.5	20.25
1	S1-4	60% CA + 40% DT	9.57	10.89
1	S1-5	50% CA + 50% DT	0.967	3.16
1	S1-6	40% CA + 60% DT	0.852	3.07
1	S1-7	30% CA + 70% DT	0.37	0.26
2	S2	54% CA + 46% DT	–	–

there is no standardized method to measure the exudation of granular FSPCM itself. A simple but effective method, the diffusion-oozing testing was taken as to be applied to determine the exudation stability of FSPCM [21, 29]. Before testing, we keep samples solidifying completely in refrigerator at 0 °C for 1 h. Then, 3 g composites were weighed in turn. And moderate composites (about 3g) were pressed in the 30 mm mold at 12 Mpa for 3 min before testing [30]. The leakage experiments of CA/DT composites were tested in a constant humidity magnetic stirrer apparatus. Finally, the made-up samples were heated for 60 s at 60 °C to test and observe their leakage. The leakage ratio in Table 1 is mass of leaked CA divided by total mass of CA in the corresponding composites [22]. Afterward, the main testing sample was marked as S2 in the following text.

Results and discussion

Experimental phenomenon and results of leakage tests

The preparation process of composites is shown in Fig. 1. And the results of leakage test are exhibited in Fig. 2. Figures 1 and 2 show that there was liquid CA left in the beaker in Fig. 1a–d, more or less. CA was not fully absorbed into the porous space of DT in Fig. 1a–d, since the CA/DT composites showed a significant amount of CA leakage during the heating process. Under the condition of high temperature, the CA/DT composites could not remain form stable because the "glue" mixture was gone in different directions, respectively. Compared with Fig. 1a–d, only very much smaller amount of CA is found in Fig. 1e–f, and there is almost no imprint. It could be observed that no trace of CA leakage is observed in Fig. 1g, even if the composite was heated. It can be concluded that the composite in Fig. 1g was FSPCM without any leakage. As shown in Fig. 2, with increasing mass fraction of DT in composite, the area of leakage of the same shape in the filter paper becomes smaller and smaller. Figures 1 and 2 show the leakage test results obtained for the composite samples with impregnation ratio of 80, 70, 60, 50 40 and 30 mass%. As can be clearly seen from the photographs, the composite with 50 mass% CA starts to exhibit little leakage of CA liquid. However, the leakage of CA can be ignored. And the composite PCM shows a little or no leakage behavior as long as the impregnation ratio of CA was equal to or lower as the form-stable combination ratio, 50 mass%. It confirms that CA has been successfully loaded with DT support. It also may be concluded that the mass fraction 50% of DT can prevent the leakage of CA and form the FSPCM. Taking into accounting latent heat, leakage ratio and economy cost, the sample S2 was selected as the main testing sample in the following text.

At the same conditions, the flow speed gets slowly with the increase in DT content. It may be caused by the high viscosity of composite mixture in the experiment process. The area of every sample was measured by a ruler. The results are also listed in Table 1 and shown in Fig. 3. From Fig. 3, the leakage area of samples is proportional to the mass fraction of DT in the composites. It can be seen that there is a good linear relationship between leakage area of composite and mass fraction of DT ($Y = -0.4887X + 32.1352$, $R^2 = 0.9449$, where Y stands for the leakage area of sample, cm^{-2} and X stands for the mass fraction of sample, %). The porous supporting minerals can provide mechanical strength to composite and also prevent the leakage of liquid PCM during phase change process. What is more, it is noted that the appropriate proportion between PCM and supporting material should be determined.

To analyze the mechanism of package influenced by DT, the leakage diagram of CA and force changes during heating process is shown in schematic diagram (Fig. 4). The mechanism of preventing CA leakage in CA/DT composite can be described in schematic diagram (Fig. 5) and confirmed by the above leakage phenomena.

As shown in Fig. 4, taking the several CA granules as the object, it is subjected to gravity force and support force

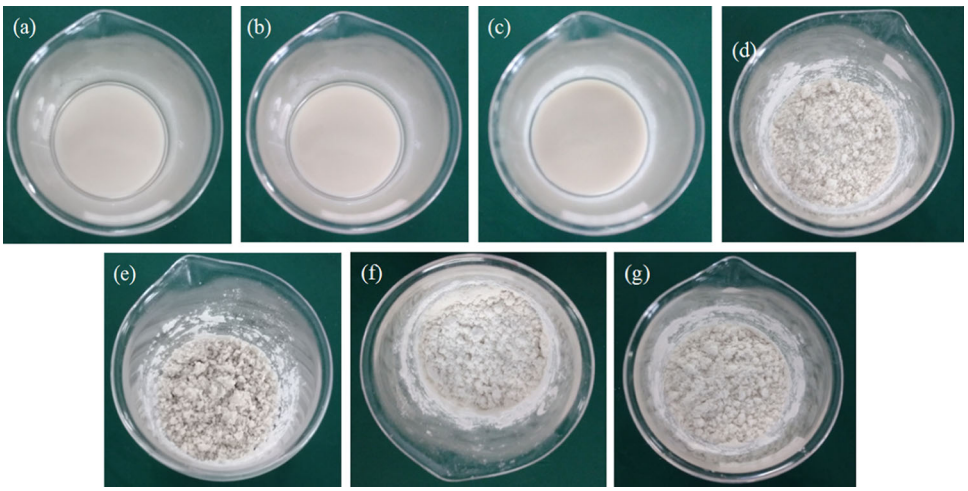

Fig. 1 Preparation process of the CA/DT composites

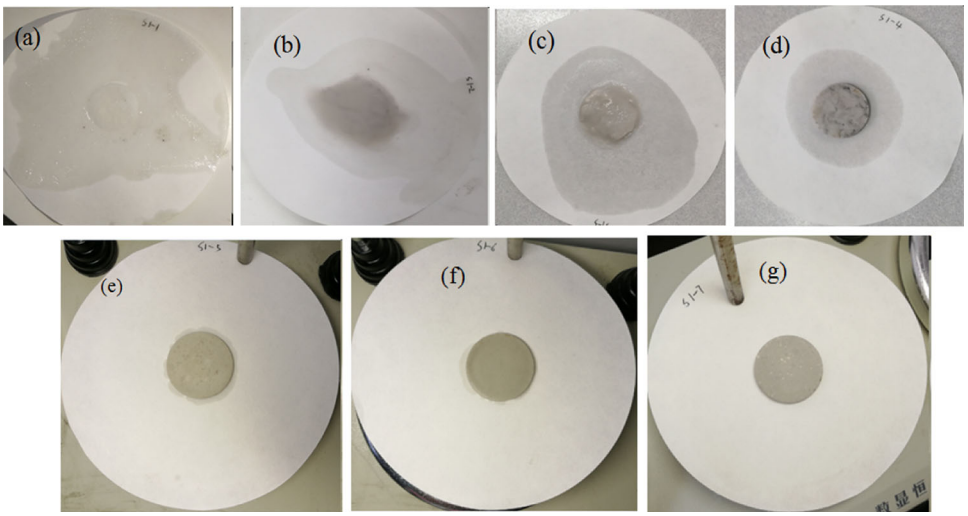

Fig. 2 Leakage test of the CA/DT composites

under solidification of CA. With the increment of heat temperature, the research object started to melt and deform. The research subject is subjected to gravity force, support force, drag force, friction force and interface force. Generally speaking, drag force is related to viscosity which is the inherent property of liquid and affected by temperature. With the increment of mass fraction of DT, the viscosity gets small, while the drag force becomes large. Interface force is determined by wettability (characterized by contact angle, e.g., capillary force) and porous specific surface area (provided by supporting materials). Tension force is closely connected to wettability (characterized by contact angle) and temperature. Only in this way the previous balance of the object was destroyed. Once the forces balance was broken, the "glue" mixture was exuded in a certain direction or some directions. Therefore, the CA liquid also begins leakage. With the temperature further increasing, drag force, friction force and interface force would increase; the leakage got more serious due to the influence of thermal expansion. However, when DT was used as the supporting matrix, like a container, it can change the heat transfer direction and increase heated area during the melting/solidifying process. In particular, the addition of DT supporting material with high thermal conductivity could improve the heat transfer efficiency by the channel among the adjacent walls and increase the friction fore between liquid CA and pore channel of DT. In Fig. 5, G stands for gravity force; N stands for support force; F_f stands for friction force; F_d stands for drag force; F_{lt} stands for capillary force; F_{rt} stands for tension force. As shown in Fig. 5a, b, in the initial heating period, the joint force in the direction of being vertical to the pore

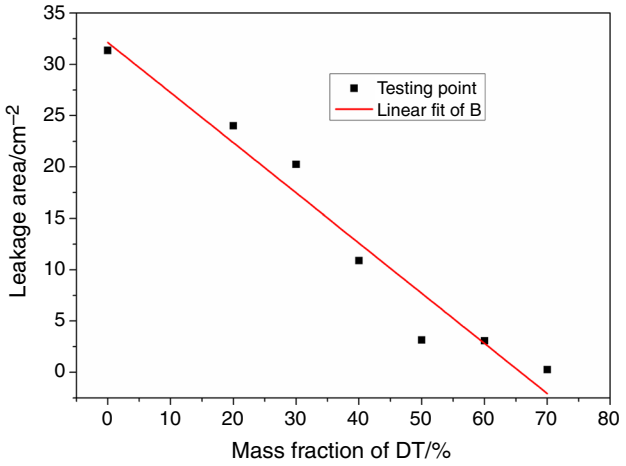

Fig. 3 Leakage area of different mass fractions of DT in the CA/DT composites

channel is small and could be ignored. With the increase in the temperature, the joint force in the direction which is vertical to the pore channel is larger than that of the direction which is parallel to the pore channel. As a result, even though the research object in the DT is further heated, there is forces balance among the comprehensive effects of drag force of liquid PCM, capillary force, surface tension force and gravitational force. The liquid CA is extension without leakage in the pore channel of DT. So the leakage of PCMs is prevented when the above balance relationships are not broken. In a word, except for the inherent condition factors, choosing the suitable porous supporting material, PCM and the optimal proportion between them become the key factor to fabricate the FSPCM [22].

Chemical compatibility of the CA/DT FSPCM

With regard to the development of FSPCM via impregnation into a solid supporter, chemical compatibility is one of the crucial factors [31], so the chemical compatibility of between CA and DT was determined via FTIR. The spectra of CA, DT and CA/DT composite of S2 are shown in Fig. 6. As can be seen in the spectrum of CA, the typical asymmetric stretching vibration at 1710 cm^{-1} is ascribed to the C=O group. The bands at 939 and 1410 cm^{-1} correspond to –OH bending vibration of CA. The –CH_3 and –CH_2 symmetric stretching vibration is found at 2850 and 2930 cm^{-1}, respectively. In the spectra of DT, the peak at 471 cm^{-1} indicates the asymmetric stretching vibration of Si–O group; the asymmetric stretching vibration peak at 793 cm^{-1} represents the vibration of SiO–H group; the peak around 1090 cm^{-1} belongs to the asymmetric stretching vibration of siloxane (–Si–O–Si–) group. All of these characteristic peaks suggest that diatomite is mainly composed of SiO_2. The bands at 2850 and 2920 cm^{-1} stand for –OH group, and it means there is H_2O in DT. The characteristic peaks CA and DT were both included in the FTIR spectrum of CA/DT composite. Furthermore, no other new peaks occurred and only few changes in wavenumbers were observed. All the main absorption peaks of both CA and DT occurred as predicted. According to FTIR results, we can conclude that no chemical interaction occurs between CA and DT support, while some physical interactions exit, including hydrogen bonding interactions, capillary effect and surface tension forces. These physical interactions might result in the peak shifts and contribute to the shape stabilization of FSPCM because

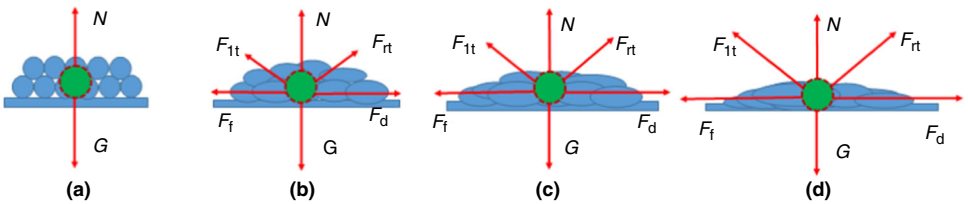

Fig. 4 Leakage diagram of CA and force changes during heating process

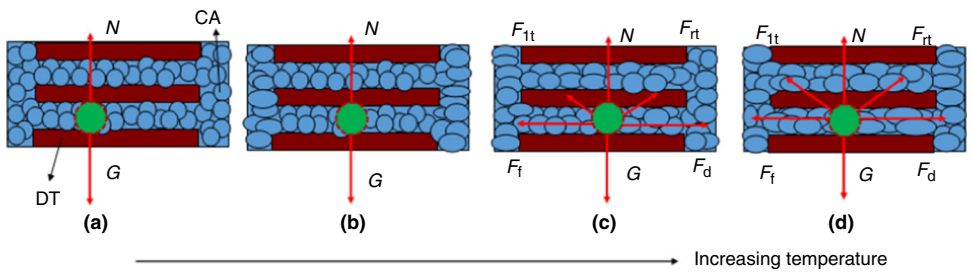

Fig. 5 Mechanism diagram of preventing CA leakage in CA/DT composite

the CA molecules are firmly tied to developed pores of DT by the confinement effect.

The morphology of the CA/DT FSPCM

Figure 7 shows the SEM images of pure CA, DT and CA/DT FSPCM. Figure 7a shows the pure CA takes on the pure white glue. As shown in Fig. 7b, the "pancake" structure of DT can be clearly seen to have a great number of porous holes in the surface, as expected. Figure 7c reveals the surface of the DT's "pancake" structure can be well covered and randomly distributed by the impregnated CA. Moreover, it can be found that pure CA was embedded in the porous holes of DT. And Fig. 7c displays the most of surface holes of DT have been covered. It demonstrates that the CA can be greatly absorbed in the DT's holes. In the other hands, the good structural stability of CA/DT could prevent the leakage of the CA and make it suitable for the application in TES system.

Thermal properties of CA/DT PCM composite

As the critical factors of PCMs, the phase change temperature and thermal enthalpy are considered as the key data to evaluate the thermal properties of PCMs. Therefore, these key data of composites were determined by DSC method. The DSC curves of CA and CA/DT are exhibited in Fig. 8. The thermal properties of the samples obtained from the DSC are presented in Table 2. As shown in Fig. 8, the melting temperature and thermal enthalpy of pure CA are 35.9 °C and 169.5 J g^{-1}, respectively. The phase change behaviors of composites are similar to that of the pure CA. However, after DT was added into pure CA to be employed as the supporting material, the phase change enthalpy values of CA/DT with different contents of CA were reduced from 169.5 to 47.7 J g^{-1}. On the other hand, the higher the mass ratio of DT, the smaller the latent heat of the composites.

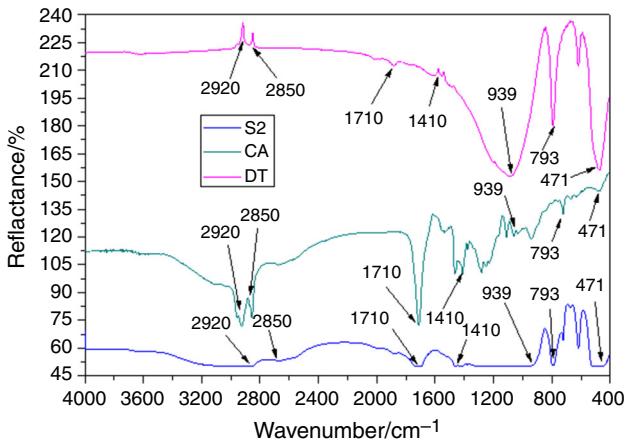

Fig. 6 FTIR spectra of CA, DT and CA/DT PCM

What is more, in some studies [32–34], the crystallinity value (CV) which is closely related to thermal energy storage is usually to taken to be as a key parameter of composite PCMs. Therefore, the crystallinity value was employed to characterize the slope of the mathematical fitting in this work.

CV can be calculated by the following formula:

$$\mathrm{CV}_{\mathrm{CA}} = \frac{\Delta H_{\mathrm{m}}}{\beta \times \Delta H_{\mathrm{pure}}}$$

where ΔH_{m} is the measuring melting enthalpy of CA/DT composites. ΔH_{pure} stands for the melting enthalpy of pure CA. β refers to the mass fraction of CA in CA/DT composites.

The measuring enthalpy values and calculating enthalpy values of CA/DT composites were fitted by a simple linear model. It can be seen that the measuring enthalpy values and calculating enthalpy values showed a good linear relationship. The mathematical fitting results are shown in Fig. 9. And the relationship can be easily drawn out as the following model by mathematical fitting: $\Delta H_{\mathrm{m}} = -7.4473 + 1.0383 \times \beta \times \Delta H_{\mathrm{pure}}$ ($R^2 = 0.9927$).

Besides, it can be seen that the phase change temperature of CA in the composite CA/DT decreased from 35.9 to 34.0 °C during the melting process. There are two possible reasons for this phenomenon. Firstly, the DT has higher thermal conductivity compared with pure CA, and it might improve the heat transfer rate to a certain extent; secondly, it may be attributed to the physical and weak interaction between CA and porous wall of DT. But the effect on the solidifying process is not significant. Such minor difference is probably caused by the physical interactions implied in FTIR analysis. Considering that the proper thermal comfort application in building is 10–40 °C, it again demonstrates that CA/DT FSPCM is more suitable to be taken as the PCMs used in thermal energy storage system for buildings.

Thermal stability of CA/DT FSPCM

It is also the important performance to choose PCM with suitable thermal stability, when the ambient temperature is higher than work temperature. Therefore, the thermal stability of the representative samples was determined by TG. The TG curve of CA and CA/DT FSPCM is presented in Fig. 10. As shown in Fig. 10, the mass loss of pure CA starts at around 90 °C and ends around 230 °C, while the starting temperature and the ending temperature of composite sample are 130 °C and 240 °C, respectively. There is about 99.92% mass loss of CA after 300 °C. However, the mass loss of the FSPCM is about 51.26%, even if the heating temperature is up to 320 °C. The results represent

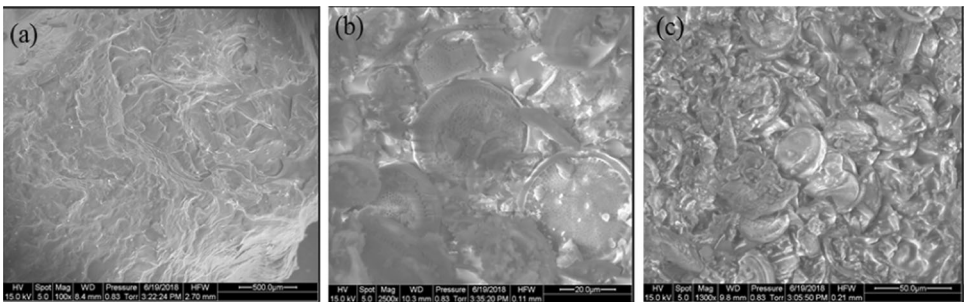

Fig. 7 SEM photographs of CA, DT and CA/DT FSPCM

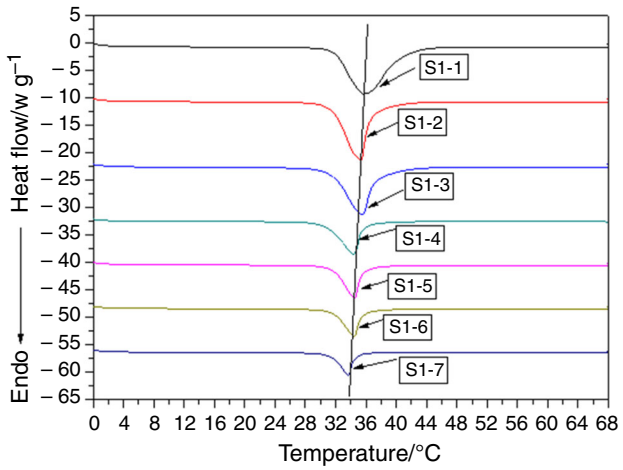

Fig. 8 DSC curve CA and CA/DT composites

that the thermal stability of the CA/DT FSPCM is much better than that of the pure CA. So the CA/DT FSPCM has good thermal stability and was more suitable used in thermal energy storage in building applications.

The cooling curve of the CA/DT FSPCM

The improvement in thermal conductivity of FSPCM was verified by comparing its melting and freezing performance before and after DT addition by cooling curve tests. Figure 11 shows the cooling curve of CA and CA/DT FSPCM.

The melting time was taken as a time elapsed from the same initial temperature (− 12 °C) to the melting point of pure CA (26.7 °C). The solidification time was taken as a time elapsed from the same initial temperature (33.6 °C) to below the freezing point of pure CA (24 °C). As shown in Fig. 11, the melting process took about 9 min for pure CA, whereas it only took about 3.5 min for CA/DT composites of S1-3. During solidification period, the freezing time took 14 min for pure CA and less than 10 min for CA/DT composites of S1-3. The composites display obviously faster heat storage and release rates than that of pure CA. In addition, Fig. 11 also shows that the pure CA has obvious temperature plateaus in the heating and cooling process. The results indicate the DT addition increase in the heat transfer rate in the composites. It again demonstrates heat transfer efficiency of the composites be enhanced significantly by DT. This is in good agreement with the conclusion in the above discussion. The reasons may be that

Table 2 Phase temperatures and latent heat values of CA and CA/DT composites

Sample	Mass fraction of CA/%	Melting temperature/°C	latent heat of melting/ J g^{-1}	Solidifying temperature/°C	Latent heat of solidifying/J g^{-1}
S1-1	100	35.9	169.5	26.8	167.6
S1-2	80	35.4	135.6	27.7	138.1
S1-3	70	35.4	116.9	26.9	118.3
S1-4	60	34.9	91.4	27.3	91.7
S1-5	50	34.9	78.9	27.0	79.8
S1-6	40	34.8	65.0	26.8	66.0
S1-7	30	34.0	47.7	27.0	49.0
S2	54	34.9	89.2	27.2	89.3
CA + expanded perlite [35]	55	31.8	98.1	31.6	98.1
CA + halloysite [36]	60	29.34	75.52	25.28	75.52

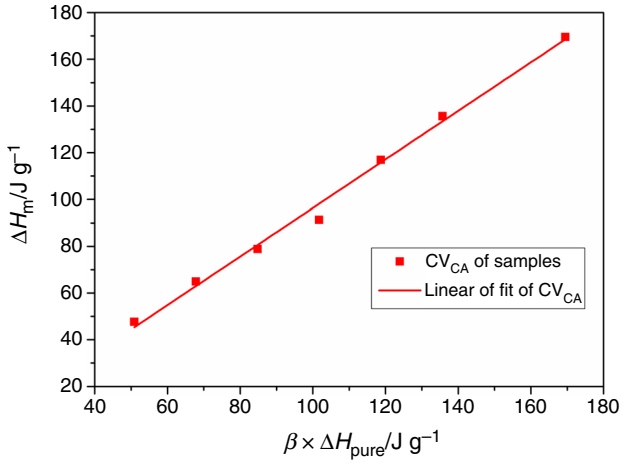

Fig. 9 Relationship between measuring enthalpy values and calculating enthalpy values of CA/DT composites

thermal conductivity of DT is higher than that of pure CA, and larger quantities of connection channels in multi-walls of DT provide the heat conduction path for the pure CA. What is more, it can be found that both the melting time and the freezing time become shorter and shorter with the increment in mass fraction of DT in composite. In addition, the stability of the phase change material was also tested and supplemented using cyclic test in which 120 heating and cooling cycles are repeated taking advantage of the selected sample S2. The comparison between before and after heating and cooling cycles is shown in Fig. 12. As shown in Fig. 12, comparing the DSC results of S2 before heating and cooling cycles with those of S2 after heating and cooling cycles, there is no significant difference of the phase change temperature and latent heat value during the melting and solidifying processes. Though a long life cycles, CA/DT FSPCM has good thermal stability and reliability.

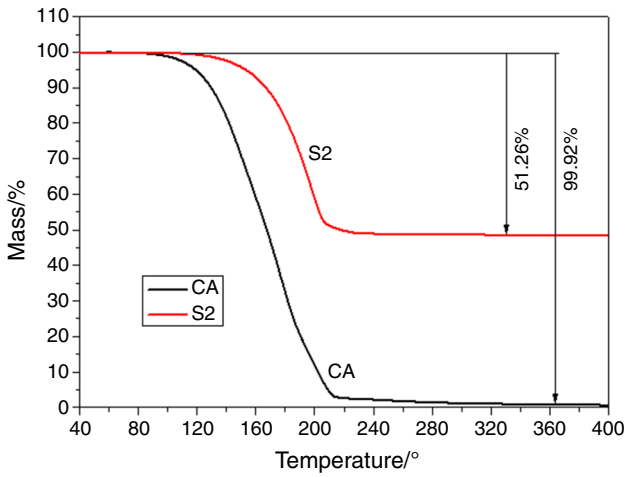

Fig. 10 TG curve CA and CA/DT FSPCMs

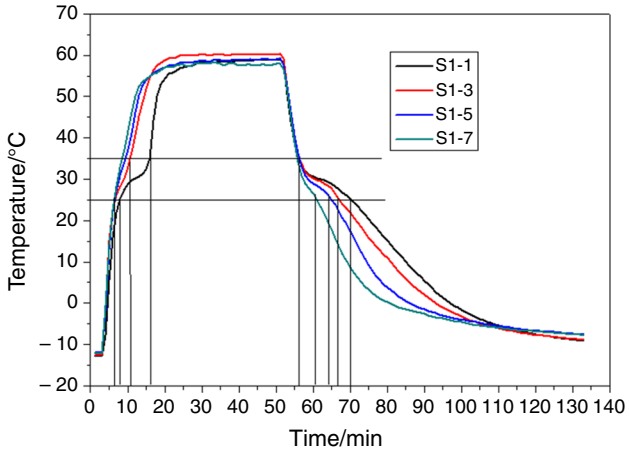

Fig. 11 Cooling curve CA and CA/DT composites

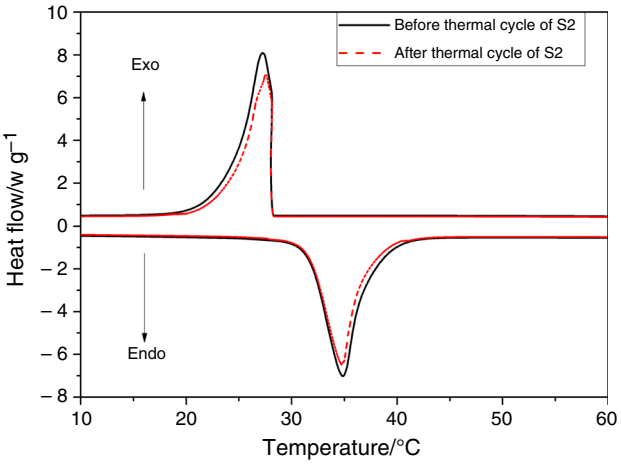

Fig. 12 DSC curve of CA/DT FSPCM before and after 120 heating and cooling cycles

Conclusions

In this study, the DT was employed to load CA and prepared CA/DT FSPCM via the direct impregnation method. The leakage, chemical compatibility, morphology, thermal properties and the thermal storage and release properties of CA/DT FSPCM were investigated. According to the research mentioned above, the conclusions can be drawn as follows:

1. The addition DT can prevent the liquid leakage of organic PCMs. There is a good linear relationship between leakage area of composites and mass fraction of DT($Y = -0.4887X + 32.1352$, $R^2 = 0.9449$). When the mass fraction of DT is equal to or lower as the form-stable combination ratio, 50 mass%, there is no leakage of liquid CA for CA/DT FSPCM. Moreover, the mechanism of preventing leakage of liquid

CA was obtained that the forces balance of liquid CA could not be broken with the addition of DT.

2. FTIR results indicate that the CA/DT FSPCM has good chemical compatibility. The morphology of the CA/DT FSPCM also demonstrates that the prepared CA/DT FSPCM was achieved and the DT with developed pore space is the quite suitable supporting materials for the PCM.
3. Because pure CA was absorbed into porous structure of DT, the CA/DT PCMS was confirmed the composite has better thermal stability than that of pure CA by TG analysis and heating and cooling cycles. There is a good linear relationship between the measuring enthalpy values and calculating enthalpy values of CA/DT composites ($\Delta H_m = -7.4473 + 1.0383 \times \beta \times \Delta H_{pure}$ ($R^2 = 0.9927$)). When CA mass content is 50% in the CA/DT composites, the melting temperature and solidifying temperature of composite samples are 34.9 °C and 27.0 °C, respectively. Correspondingly, the latent heats of the composite are 78.9 J g^{-1} and 79.8 J g^{-1}. The improvement in thermal conductivity of FSPCM was verified by comparing its melting and freezing performance before and after DT addition. The DT not only can be taken as the support materials, but also can play the role in enhancing the heat transfer efficiency of the composite.

In a word, the CA/DT FSPCM has a good application prospect in the field of building, due to its good thermophysical properties. However, the mass ratios depend on the comprehensive factors such as leakage, latent heat and working temperature. Besides, the heat conductivity should be paid more attention in the future work.

Acknowledgements This work is supported by the National Natural Science Foundation of China (41872039 and 41831285), Hebei Key Technology R&D Program of the Agency of Hebei Province (17214016), the Open Project of State Key Laboratory Cultivation Base for Nonmetal Composites and Functional Materials (17kffk13), the One-Thousand-Talents Scheme in Sichuan Province, Sichuan Science and Technology Program (2018JY0462), Hebei outstanding young scholars, Longshan Fund of Southwest University of Science and Technology (17QR004), the Opening Project of Material Corrosion and Protection Key Laboratory of Sichuan Province (2018CL20) and PhD Research Startup Foundation of Hebei GEO University (BQ2017020, BQ2017021).

References

1. Gu X, Qin S, Wu X, Li Y, Liu Y. Preparation and thermal characterization of sodium acetate trihydrate/expanded graphite composite phase change material. J Therm Anal Calorim. 2016;125(2):831–8. https://doi.org/10.1007/s10973-016-5444-4.
2. Wen R, Jia P, Huang Z, Fang M, Liu Y, Wu X, et al. Thermal energy storage properties and thermal reliability of PEG/bone char composite as a form-stable phase change material. J Therm Anal Calorim. 2018;132(3):1–9. https://doi.org/10.1007/s10973-017-6934-8.
3. Sarı A, Karaipekli A. Preparation, thermal properties and thermal reliability of capric acid/expanded perlite composite for thermal energy storage. Mater Chem Phys. 2008;109(2):459–64. https://doi.org/10.1016/j.matchemphys.2007.12.016.
4. Mei D, Zhang B, Liu R, Zhang Y, Liu J. Preparation of capric acid/halloysite nanotube composite as form-stable phase change material for thermal energy storage. Sol Energy Mater Sol Cells. 2011;95(10):2772–7. https://doi.org/10.1016/j.solmat.2011.05.024.
5. Karaipekli A, Sarı A. Capric–myristic acid/expanded perlite composite as form-stable phase change material for latent heat thermal energy storage. Renew Energy. 2008;33(12):2599–605. https://doi.org/10.1016/j.renene.2008.02.024.
6. Jamekhorshid A, Sadrameli SM, Farid M. A review of microencapsulation methods of phase change materials (PCMs) as a thermal energy storage (TES) medium. Renew Sustain Energy Rev. 2014;31(2):531–42. https://doi.org/10.1016/j.rser.2013.12.033.
7. Fang Y, Liu X, Liang X, Liu H, Gao X, Zhang Z. Ultrasonic synthesis and characterization of polystyrene/n-dotriacontane composite nanoencapsulated phase change material for thermal energy storage. Appl Energy. 2014;132(11):551–6. https://doi.org/10.1016/j.apenergy.2014.06.056.
8. Tumirah K, Hussein MZ, Zulkarnain Z, Rafeadah R. Nano-encapsulated organic phase change material based on copolymer nanocomposites for thermal energy storage. Energy. 2014;66(4):881–90. https://doi.org/10.1016/j.energy.2014.01.033.
9. Khadiran T, Hussein MZ, Zainal Z, Rusli R. Encapsulation techniques for organic phase change materials as thermal energy storage medium: a review. Sol Energy Mater Sol Cells. 2015;143:78–98. https://doi.org/10.1016/j.solmat.2015.06.039.
10. Sarı A. Fabrication and thermal characterization of kaolin-based composite phase change materials for latent heat storage in buildings. Energy Build. 2015;96:193–200. https://doi.org/10.1016/j.enbuild.2015.03.022.
11. Liu S, Yang H. Composite of coal-series kaolinite and capric-lauric acid as form-stable phase-change material. Energy Technol. 2015;3(1):77–83. https://doi.org/10.1002/ente.201402125.
12. Lv P, Liu C, Rao Z. Review on clay mineral-based form-stable phase change materials: preparation, characterization and applications. Renew Sustain Energy Rev. 2017;68:707–26. https://doi.org/10.1016/j.rser.2016.10.014.
13. Sobolciak P, Karkri M, Al-Maadeed MA, Krupa I. Thermal characterization of phase change materials based on linear low-density polyethylene, paraffin wax and expanded graphite. Renew Energy. 2016;88:372–82. https://doi.org/10.1016/j.renene.2015.11.056.
14. Liu S, Han L, Xie S, Jia Y, Sun J, Jing Y, et al. A novel medium-temperature form-stable phase change material based on dicarboxylic acid eutectic mixture/expanded graphite composites. Sol Energy. 2017;143:22–30. https://doi.org/10.1016/j.solener.2016.12.027.
15. Karaipekli A, Biçer A, Sarı A, Tyagi V. Thermal characteristics of expanded perlite/paraffin composite phase change material with enhanced thermal conductivity using carbon nanotubes. Energy Convers Manag. 2017;134:373–81. https://doi.org/10.1016/j.enconman.2016.12.053.
16. Karaipekli A, Sarı A. Preparation, thermal properties and thermal reliability of eutectic mixtures of fatty acids/expanded vermiculite as novel form-stable composites for energy storage. J Ind Eng Chem. 2010;16(5):767–73. https://doi.org/10.1016/j.jiec.2010.07.003.
17. Jeong SG, Jeon J, Chung O, Kim S, Kim S. Evaluation of PCM/diatomite composites using exfoliated graphite nanoplatelets (xGnP) to improve thermal properties. J Therm Anal

Calorim. 2013;114(2):689–98. https://doi.org/10.1007/s10973-013-3008-4.
18. Deng Y, Li J, Qian T, Guan W, Wang X. Preparation and characterization of KNO_3/diatomite shape-stabilized composite phase change material for high temperature thermal energy storage. J Mater Sci Technol. 2016;2:198–203. https://doi.org/10.1016/j.jmst.2016.02.011.
19. Liu Z, Hu D, Lv H, Zhang Y, Wu F, Shen D, et al. Mixed mill-heating fabrication and thermal energy storage of diatomite/paraffin phase change composite incorporated gypsum-based materials. Appl Therm Eng. 2017;118:703–13. https://doi.org/10.1016/j.applthermaleng.2017.02.057.
20. Ramakrishnan S, Sanjayan J, Wang X, Alam M, Wilson J. A novel paraffin/expanded perlite composite phase change material for prevention of PCM leakage in cementitious composites. Appl Energy. 2015;157:85–94. https://doi.org/10.1016/j.apenergy.2015.08.019.
21. Li X, Chen H, Liu L, Lu Z, Sanjayan JG, Duan W. Development of granular expanded perlite/paraffin phase change material composites and prevention of leakage. Sol Energy. 2016;137:179–88. https://doi.org/10.1016/j.solener.2016.08.012.
22. Ramakrishnan S, Wang X, Sanjayan J, Wilson J. Assessing the feasibility of integrating form-stable phase change material composites with cementitious composites and prevention of PCM leakage. Mater Lett. 2017;192:88–91. https://doi.org/10.1016/j.matlet.2016.12.052.
23. Li H, Chen H, Li X, Sanjayan JG. Development of thermal energy storage composites and prevention of PCM leakage. Appl Energy. 2014;35:225–33. https://doi.org/10.1016/j.apenergy.2014.08.091.
24. Han J, Liu S. Myristic acid-hybridized diatomite composite as a shape-stabilized phase change material for thermal energy storage. RSC Adv. 2017;7(36):22170–7. https://doi.org/10.1039/C7RA02385E.
25. Wen R, Zhang X, Huang Z, Fang M, Liu Y, Wu X, et al. Preparation and thermal properties of fatty acid/diatomite form-stable composite phase change material for thermal energy storage. Sol Energy Mater Sol Cells. 2018;178:273–9. https://doi.org/10.1016/j.solmat.2018.01.032.
26. Sarı A, Bicer A, Al-Sulaiman FA, Karaipekli A, Tyagi V. Diatomite/CNTs/PEG composite PCMs with shape-stabilized and improved thermal conductivity: preparation and thermal energy storage properties. Energy Build. 2018;164:166–75. https://doi.org/10.1016/j.enbuild.2018.01.009.
27. Fu X, Liu Z, Xiao Y, Wang J, Lei J. Preparation and properties of lauric acid/diatomite composites as novel form-stable phase change materials for thermal energy storage. Energy Build. 2015;104:244–9. https://doi.org/10.1016/j.enbuild.2015.06.059.
28. Li C, Fu L, Ouyang J, Tang A, Yang H. Kaolinite stabilized paraffin composite phase change materials for thermal energy storage. Appl Clay Sci. 2015;115:212–20. https://doi.org/10.1016/j.clay.2015.07.033.
29. Li B, Nie S, Hao Y, Liu T, Zhu J, Yan S. Stearic-acid/carbon-nanotube composites with tailored shape-stabilized phase transitions and light–heat conversion for thermal energy storage. Energy Convers Manag. 2015;98:314–21. https://doi.org/10.1016/j.enconman.2015.04.002.
30. Lv P, Liu C, Rao Z. Experiment study on the thermal properties of paraffin/kaolin thermal energy storage form-stable phase change material. Appl Energy. 2016;182:475–87. https://doi.org/10.1016/j.apenergy.2016.08.147.
31. Goitandia AM, Beobide G, Aranzabe E, Aranzabe A. Development of content-stable phase change composites by infiltration into inorganic porous supports. Sol Energy Mater Sol Cells. 2015;134:318–28. https://doi.org/10.1016/j.solmat.2014.12.010.
32. Liu S, Yang H. Stearic acid hybridizing coal-series kaolin composite phase change material for thermal energy storage. Appl Clay Sci. 2014;101:277–81. https://doi.org/10.1016/j.clay.2014.09.002.
33. Gu X, Liu P, Bian L, Peng L, Liu Y, He H. Mullite stabilized palmitic acid as phase change materials for thermal energy storage. Minerals. 2018;8(10):440–50. https://doi.org/10.3390/min8100440.
34. Su X, Jia S, Lv G, Yu D. A unique strategy for polyethylene glycol/hybrid carbon foam phase change materials: morphologies, thermal properties, and energy storage behavior. Materials. 2018;11:2011–27. https://doi.org/10.3390/mal1102011.
35. Sarı A, Karaipekli A. Preparation, thermal properties and thermal reliability of capric acid/expanded perlite composite for thermal energy storage. Mater Chem Phys. 2008;109(2):459–64. https://doi.org/10.1016/j.matchemphys.2007.12.016.
36. Mei D, Zhang B, Liu R, Zhang Y, Liu J. Preparation of capric acid/halloysite nanotube composite as form-stable phase change material for thermal energy storage. Sol Energy Mater Sol Cells. 2011;95(10):2772–7. https://doi.org/10.1016/j.solmat.2011.05.024.